Narrow-Bandwidth Spontaneous Luminescence from Oriented Semiconducting Polymer Nanostructures

P. Kumar,[†,‡] A. Mehta,[†,§] M. D. Dadmun,[‡] J. Zheng,[||] L. Peyser,[||] A. P. Bartko,[||] R. M. Dickson,[||] T. Thundat,[§] B. G. Sumpter,[⊥] D. W. Noid,[⊥] and M. D. Barnes*[,#]

Department of Chemistry, University of Tennessee, Knoxville, Tennessee 37830, School of Chemistry and Biochemistry, Georgia Institute of Technology, Atlanta, Georgia 30332-0400, Life Sciences Division, Oak Ridge National Laboratory, Oak Ridge, Tennessee 37831-6142, Computer Sciences and Mathematics Division, Oak Ridge National Laboratory, Oak Ridge, Tennessee 37831-6142, and Chemical Sciences Division, Oak Ridge National Laboratory, Oak Ridge, Tennessee 37831-6142

Received: January 15, 2003; In Final Form: April 21, 2003

High-resolution fluorescence imaging of isolated nanoparticles of a common semiconducting polymer (poly-[2-methoxy-5-(2′-ethyl-hexyloxy)-1,4-phenylene vinylene, MEH-PPV), produced by ink-jet printing techniques, has revealed highly uniform transition moment orientation *perpendicular* to the glass substrate. In contrast with the broad emission spectra associated with bulk or single molecules of these species in thin films, we observe narrow photoluminescence emission spectra (10−15 nm fwhm) from individual oriented polymer nanostructures with no evidence of spectral diffusion on time scales of several hundred seconds. The distribution of center frequencies (from several hundred individual nanoparticle measurements) shows clearly defined peaks that can be correlated with excitonic traps of integer multiples of monomer conjugation lengths (8, 9, 10, and 11). The observation of discrete emission characteristics in this important class of materials suggests exciting possibilities in photonics and molecular optoelectronics.

Introduction

Semiconducting polymers[1] are currently the subject of intense interest in the context of molecular-scale optoelectronics. Specifically, strategies to constrain molecular morphologies[2] and intramolecular organization of conjugated segments within a single polymer chain have important implications to polymer-based molecular-scale electronics[3] and control of energy transfer.[4] Although techniques for isolating and, to some extent, controlling chain organization of single molecules of conjugated polymers in thin films have become possible in recent years, [5,6] engineering highly aligned chain ordering in conventional thin-film processing is quite difficult because there are significant entropic and kinetic barriers that must be overcome. While a number of interesting fluorescence polarization anisotropy measurements on single semiconducting polymer molecules point to compact ordered geometries in polymer-supported thin films,[6,7,15] these species almost always show randomly oriented (in-plane) transition moment orientation with broad emission spectra similar to most molecular dyes.

Poly(phenylene vinylene) (PPV) derivatives and related materials have received a great deal of attention in polymer-based optoelectronic device contexts because of their efficient luminescence and charge transport properties, as well as the convenience in solution-phase processing afforded by side-chain derivatization. Of these, perhaps the most widely studied is (poly[2-methoxy-5-(2′-ethyl-hexyloxy)-1,4-phenylene vinylene] or MEH-PPV. A single MEH-PPV chain is comprised of conjugated stiff-chain segments (6−12 monomer units long) connected by flexible joints, or tetrahedral defects, which allows for a variety of morphologies[8] (which in turn affect the photophysics[9]) depending on molecular weight, solvent, and thin-film host material.[4,6,10−13] Despite the structural complexity and large physical size of these species (relative to single-chromophore molecules), there is compelling spectroscopic evidence that the emission originates from highly localized regions (luminescent trap states) of the macromolecule.[12,14] On−off blinking, multiple intensity jumps, and discrete photobleaching have been observed from single chains of PPV molecules, observations that are consistent with a single (or few) localized emissive excitonic trap state. These observations have been explained by a picture of efficient excitonic excitation transfer between local quasi-chromophores within the molecule, resulting in emission from localized regions along the polymer chain. Polarization spectroscopy of single MEH-PPV molecules in thin films showed evidence of compact chain configurations in thin-film preparations,[15−17] a result interpreted as a coil−rod collapse transition[15] during solvent evaporation of the spun-cast film. However, in terms of spectral properties, spectra of single MEH-PPV molecules probed in dilute thin films are usually not significantly different from the bulk.

Here, we report observation of uniformly oriented transition moments along the *z*-axis of single MEH-PPV molecules that point to a high degree of intramolecular alignment of conjugated segments. In part because of decoupling of electronic perturbations of the substrate by virtue of the *z*-orientation, we find significant enhancement of photochemical stability, as well as narrow bandwidth spectral signatures (≤15 nm fwhm) from

* To whom correspondence should be addressed. E-mail: barnesmd1@ornl.gov.
† These authors contributed equally to this work.
‡ University of Tennessee.
§ Life Sciences Division, Oak Ridge National Laboratory.
|| Georgia Institute of Technology.
⊥ Computer Sciences and Mathematics Division, Oak Ridge National Laboratory.
Chemical Sciences Division, Oak Ridge National Laboratory.

10.1021/jp034107v CCC: $25.00
Published on Web 06/05/2003

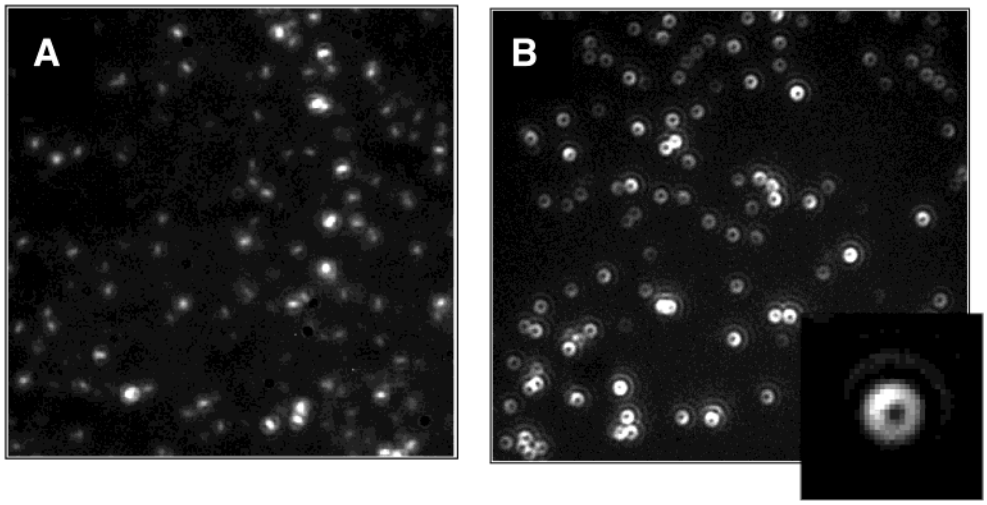

Figure 1. Comparison of emission patterns (A) from a thin film spin-coated from 10^{-11} mol/L MEH-PPV solution in THF and (B) from MEH-PPV nanoparticle samples prepared from piezoelectric microdroplet generation from the same solution. The noncentrosymmetric "cats-eye"-like patterns seen under slight defocusing in the thin-film sample are characteristic of single dipoles oriented (randomly) in the $x-y$ plane (ref 23). The "donut"-like spatial intensity patterns seen for the nanoparticle sample in panel B and in close-up at lower right (shown in focus) are preserved under slight defocusing as well and correspond to transition moment orientation in the z direction. Scaling of nanoparticle coverage with MEH-PPV concentrations as low as 10^{-14} mol/L indicate that the nanoparticles are single MEH-PPV molecules.

these species. Time-resolved spectral monitoring of the fluorescence from individual nanoparticles shows highly stable emission spectra with no indication of spectral diffusion or center frequency fluctuations during the photochemical lifetime (typically several hundred seconds). The histogram of photoluminescence emission (PLE) center frequencies obtained from several hundred individual nanoparticle measurements shows discrete peaks that can be correlated with excitonic traps of integer multiples of monomer conjugation lengths ($L = 8$, 9, 10, and 11). In addition to straightforward on-demand production and spatial manipulation capability, observation of discrete luminescence properties in this important class of materials suggests several exciting possible applications in photonics and molecular-scale optoelectronics.

Experimental Section

We used ink-jet printing methods to isolate single conducting polymer chains in microdroplets of solution typically less than 5-μm initial diameter that evaporate en route to the coverglass substrate. Used extensively in our laboratory (ORNL) for manipulation and interrogation of single-fluorescent molecules,[18] as well as for altering the phase structure of mesoscale mixed polymer systems,[19] a microdroplet format for nanoparticle production offers advantages of three-dimensional confinement without potentially complicating substrate− or support−polymer interactions. The MEH-PPV used in our experiments was obtained commercially (H. W. Sands Corp. OPA9576) without further purification and had an average molecular weight of 270 000 (polydispersity $M_n/M_w \approx 8$). Droplets of dilute MEH-PPV solution (5 μm nominal diameter and concentration of $10^{-11}-10^{-12}$ M) in doubly distilled tetrahydrofuran (THF) were generated from a piezoelectric on-demand droplet generator and dried en route to clean glass coverslips in a 20-cm vented drying tube. We found concentration-dependent nanoparticle coverage at MEH-PPV concentrations as low as 10^{-14} M indicating clearly that the polymer nanoparticles probed in our experiments are single MEH-PPV chains.

Dipole emission pattern imaging techniques were used to probe the local nature of the luminescent trap state in these species, in which optical emission (antenna) patterns are measured[20] that are uniquely defined by transition moment orientation. Recently used to probe rotational dynamics in polymer thin films[21] and single-ion emission in rare-earth-doped nanocrystals,[22] the angular anisotropy associated with single dipole emission readily distinguishes between nanoscale multichromophoric (isotropic) sources and single dipoles. In the case of the neat spun-cast film from 10^{-11} mol/L MEH-PPV solution (left) in doubly distilled THF (Figure 1a), the noncircularly symmetric "cats-eye"-like emission patterns are characteristic of single dipoles oriented (randomly) in-plane parallel to the glass substrate.[23,24] In contrast, fluorescence images from a typical nanoparticle sample produced from the same solution by piezoelectric droplet generation (Figure 1b) show "donut"-like spatial intensity patterns, which are seen in-focus, as well as for small defocusing, that are characteristic of single dipoles oriented *perpendicular* to the substrate. Sampling of individual images for precision fitting indicate that the z orientation is uniform to within 10% with a slight tilt angle of about 5° with respect to the surface normal.

Discussion and Results

Because the transition moment lies nearly collinear with the conjugation axis,[1] the uniformity in orientation evidenced by our emission pattern measurements suggests a significant degree of intramolecular order. It is difficult (but perhaps not impossible) to envision an ensemble of macromolecules each with a random disordered intramolecular structure that can produce extraordinarily uniform transition moment orientation *perpendicular to the substrate*. Figure 2 shows an example of folded polymer chain structure determined from hybrid molecular dynamics simulation. Here, a constant temperature−pressure (*NPT*) molecular dynamics simulation was used to emulate the environment of a solvated system followed by simulated annealing to emulate the rapid evaporation of the solvent. The final structure was then minimized using molecular mechanics to a rms gradient of 0.000 01. Several different initial structures were considered: a single MEH-PPV chain with 1, 2, and 3 tetrahedral defects, consisting of up to 90 monomers and multiple chains (from 7 to 20 with 16−32 monomers each) without tetrahedral defects. In all cases, the single chain folded at the sp^3 defect sites to form a cylindrical rodlike structure.

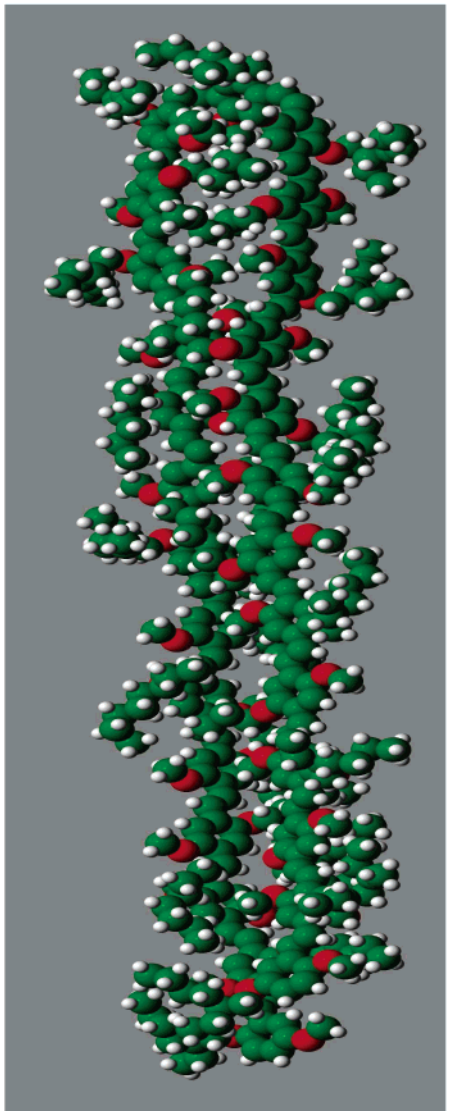

Figure 2. Molecular mechanics simulation of folded chain structure of an MEH-PPV oligomer. The minimum-energy structures are folded at sp^3 defect sites and adopt cylindrical morphologies.

The uniform *z*-orientation can be explained as a result of an electrostatic interaction between the nanoparticle (as a charged cylindrical structure) and stray charges on the glass surface. The small excess charge on the particle (typically around 10−20 electrons) is produced during droplet ejection from the quartz orifice, and the charge carriers remain on the particle after solvent evaporation.[18] If the nanostructure is cylindrical (with carriers localized on the exterior surface), the electrostatic energy is minimized by orientation of the particle with the long-axis perpendicular to the substrate surface. Further evidence of the electrostatic nature of the nanoparticle orientation was seen by probing nanoparticle orientation on grounded conducting substrates. In this case, the image charge interaction will favor orientation of the long axis parallel to the substrate, which is exactly what is observed experimentally. We find that the particle binding is extremely robust, and the samples are stable under high vacuum ($<10^{-6}$ Torr) and elevated temperatures (>200 °C), as well as over a range of ambient humidity conditions. With proper storage, we are able to reexamine individual particle samples for several months after preparation.

The structural picture suggested by molecular mechanics simulation is further supported by atomic force microscopy (AFM) results shown in Figure 3. Nanoparticle heights, probed by AFM in tapping mode (Digital Instruments Bioscope with Nanoscope IIIa controller), were measured to be within a range of 5−15 nm with an average of about 7 nm. This value is in good agreement with the persistence length of MEH-PPV measured several years ago by Heeger and co-workers using light scattering techniques.[13] Surface height images of nanoparticle samples showed individual particle images that were tip-radius-limited (≈20 nm) in the lateral dimension thus obscuring the true aspect ratio of the particles. We estimate, on the basis of the known molecular weight and hypothesized folded structure, that the aspect ratios must be between 1 and 3, depending on the chain length. The histogram of measured particle heights, shown in Figure 3, shows an approximately Gaussian distribution centered at 7.5 nm with a small number of larger (>15 nm) particles within a given sample.

Spectral properties of *z*-oriented MEH-PPV nanoparticles were investigated by dispersing emission from several particles simultaneously with a spectrograph. Because of sensitivity issues, a frame-transfer camera similar to the one used for emission pattern imaging was used to detect the wavelength-dispersed emission from the sample with the tradeoff that only a 50-nm spectral window was viewable at a time. Wavelength calibration was conveniently checked on a run-to-run basis using a europium-doped yttrium oxide nanoparticle sample[22] in which the Stark components of the $^5D_0 \rightarrow {}^7F_2$ transition (610−635 nm) provide unambiguous pixel−wavelength correspondence. Figure 4 shows a comparison of emission spectra from (A) solution-phase MEH-PPV in THF, a single in-plane MEH-PPV molecule spin-coated on glass (no support polymer) and (B) three different *z*-oriented nanoparticles (particle heights 7.2, 9.1, and 12.3 nm).[25] The relatively low signal-to-noise ratio for the single-molecule/film sample is characteristic of the poor photostability of MEH-PPV in the presence of oxygen.[16]

In contrast with bulk or in-plane single-molecule spectra, which closely resemble molecular dye fluorescence, *z*-oriented nanoparticle spectra show only a *single* narrow peak with line widths ranging from 10 to 15 nm fwhm. The line shapes are approximately Gaussian, and many individual particle spectra show some weak vibronic structure as well. Similar spectral narrowing was observed in highly ordered macroscopic PPV samples prepared by in situ polymerization by Friend and co-workers.[30] This observation provides an interesting contrast with spectral measurements made previously by Barbara and co-workers. In their experiments, different luminescent trap states were evidenced by comparing single-molecule emission spectra at successive times during illumination with a range of accessible energies observable through spectral subtraction.[16] In our case, only a *single* emissive state is accessed for the entire photochemical lifetime of the molecule. In following the spectral dynamics on a time scale of 5 frames per second, we find that there is essentially no spectral diffusion and that the emission center frequency is fixed—but *different*—for each particle.

Figure 5 shows a histogram of the peak wavelengths obtained from >350 individual nanoparticles. We see two clearly defined sharp peaks in the distribution at 608 and 613 nm with less well-defined components at 598.5 and 618 nm. The energy difference between these peaks in the center frequency distribution is in reasonable agreement with zero-order electronic energy differences between conjugation lengths, *L*, of 8, 9, and 10 monomer units ($\Delta_{8-9} = 200$ cm^{-1}, $\Delta_{9-10} = 149$ cm^{-1} $\Delta_{10-11} = 115$ cm^{-1}) calculated from $E(L) = E_0 + 2\beta \cos(\pi L/(L+1))$, where $E_0 = 34\,400$ cm^{-1} and $\beta = -8800$ cm^{-1}.[26] In terms of absolute energies, the measured data indicate lower energies per chain of 1150 cm^{-1}, which presumably derive from a LUMO

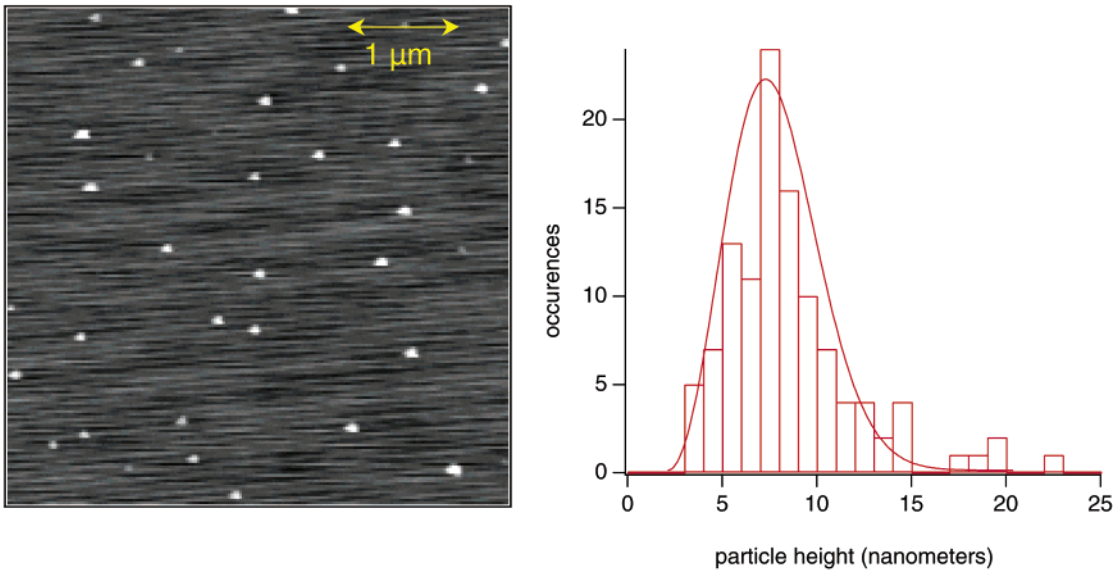

Figure 3. Typical AFM (tapping mode) surface height data (left) for MEH-PPV nanoparticles deposited on a clean glass coverslip from ultradilute (10^{-11} mol/L) microdroplets of polymer solution in doubly distilled THF. The gray levels span a *z*-range of −2 to 10 nm. Nearly all of the nanoparticles sampled show tip-radius-limited lateral extent. The right panel shows the surface height histogram obtained from 200 nanoparticles within a 10 × 10 μm^2 field of view.

lowering of the emissive chromophore by virtue of aligned conjugated segments within the core of the nanoparticle.[27] We observe a weak correlation between center frequency and spectral width, in which broadening in the single-molecule spectra appears to be associated with longer PLE center frequencies.

Even though every MEH-PPV molecule should be reasonably expected to contain a distribution of conjugated segment lengths, a single particle displays a spectrum characteristic of only *one* of them, which does not necessarily correspond to the lowest (vacuum) energy state available within the particle. In other words, why does a given particle emit with a frequency characteristic of, say, $L = 9$ frequency when it presumably has access to $L = 10$, 11, and perhaps even longer conjugation lengths. In a picture of exciton funneling to particular luminescent trap states described by Barbara and co-workers,[16] a dipole−dipole energy transfer process would seem to predict only a single peak in the center frequency distribution corresponding to the lowest singlet-exciton energy accessible within the particle. While the statistics for the PLE center frequency histogram peaks nominally at 605 and 618 are obviously not as clear as those for the two main peaks, there is a clear correlation of the cluster of these measurements with the oligomer S_1-S_0 transition energies.

We believe that the discrete distribution of center frequencies observed in photoluminescence from *z*-oriented MEH-PPV nanoparticles reflects (1) the distribution of conjugated segment lengths, (2) coupling between segments within the particle, and (3) the structural arrangement within each macromolecule/nanoparticle. In the case of a highly axially aligned chain structure, one should expect significant LUMO energy lowering for conjugated segments in the core of the particle due to favorable self-solvation effects on the protected, emissive chromophore. Solvatochromism of this type has been observed to yield shifts of more than 30 nm for green-emitting PPVs in a range of different solvents.[28] The extremes in solvation between vacuum on the outside of the nanoparticle and aligned MEH-PPV chains on the inside would lead to even more significant lowering of the HOMO−LUMO gap for any species in the particle interior. This solvatochromic shift is much larger

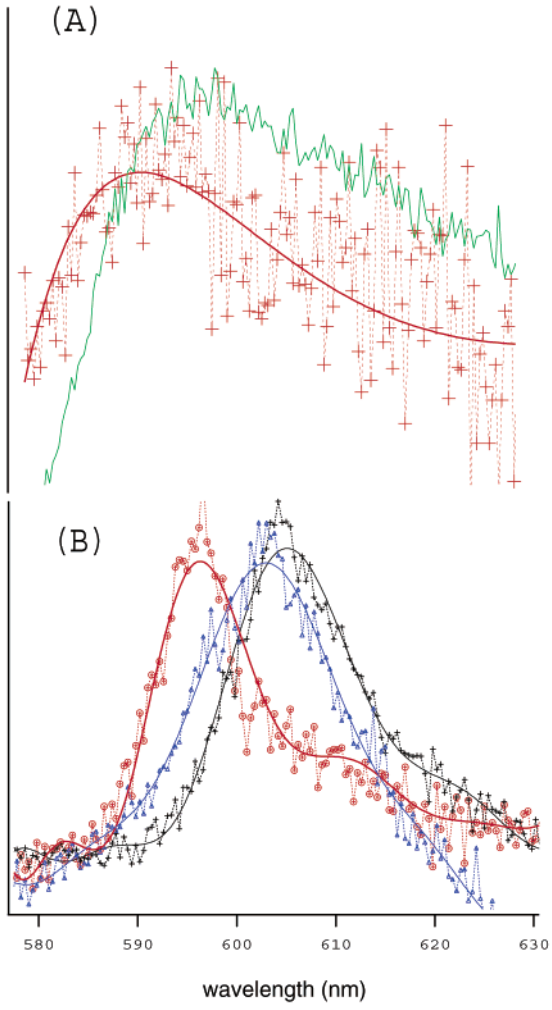

Figure 4. Comparison (A) of solution-phase (green) MEH-PPV in THF and single-molecule spectra (red lines and points) from a neat thin-film and (B) photoluminescence spectra from three different *z*-oriented MEH-PPV nanoparticles (molecules) 7, 9, and 12 nm in height as indicated from AFM measurements.

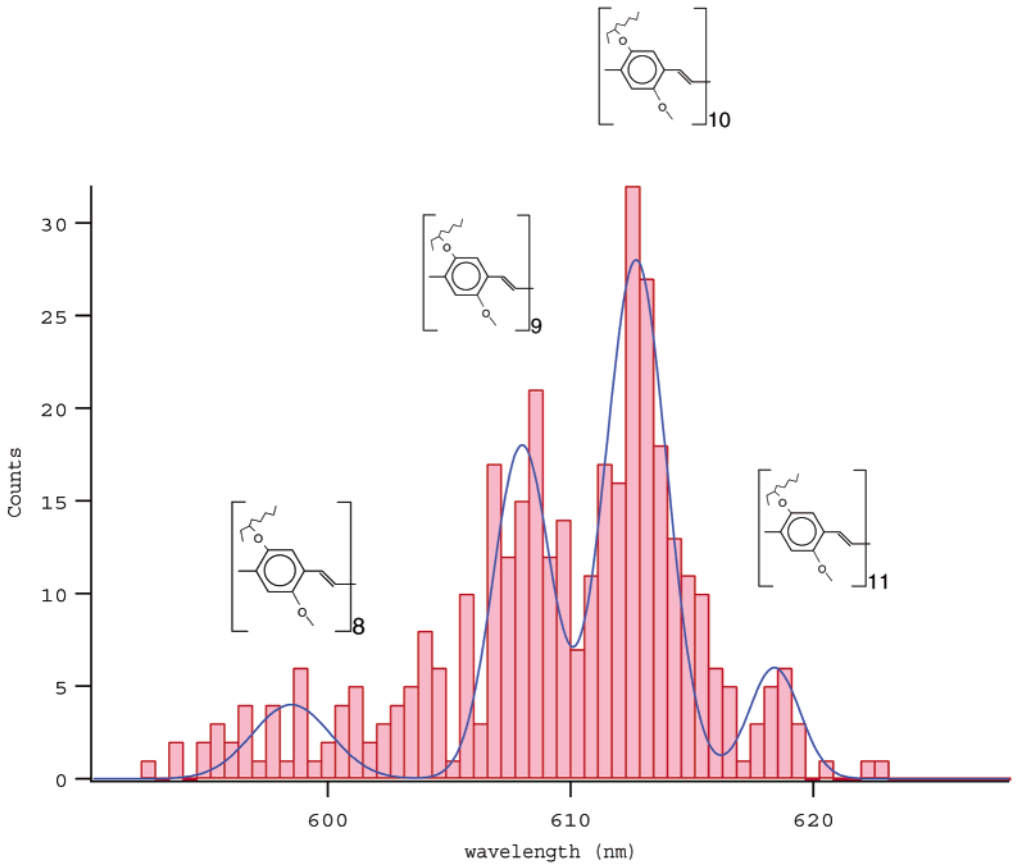

Figure 5. Histogram of center frequencies from emission spectra of *z*-oriented MEH-PPV nanoparticles (sample size = 380, bin width = 0.5 nm). The blue curve is a model function that is a sum of four Gaussian components with peak wavelengths of 598.5, 608, 612.7, and 618.5 nm. These peaks are correlated with zero-order electronic energies for 8-, 9-, 10-, and 11-mers taken from ref 26 and indicated with the inset graphics.

than the spread in HOMO−LUMO energy of different MEH-PPV chromophore conjugation lengths. Thus, depending on the structural details of each individual nanoparticle, the lowest LUMO state is always accessed with its corresponding emission frequency. As indicated by the observed distribution of nanoparticle emission center frequencies, this does not necessarily correspond to the longest conjugated segment but instead to the chromophore with the lowest energy emission due to favorable solvation effects. These results suggest that one could make a "pure color" of nanoscale particles of this class of materials if the distribution of conjugated chain lengths could be precisely controlled. Thus the color tunability would be controlled in the bulk-synthesis step and should be independent of the nanoparticle generation process.

There are several exciting applications in photonics and molecular-scale optoelectronics suggested by this work. By achieving uniform orientation perpendicular to a surface or substrate, we expect stimulated emission cross sections and lasing thresholds to be significantly enhanced in planar or whispering gallery mode resonator structures.[29] The ability to "print" single molecules with a well-defined orientation and location has important implications for optical coupling to molecular nanostructures and nanoscale optoelectronics as well. Because this technique does not require an external templating material, these kinds of conducting polymers can be printed in direct contact with other types of nanoengineered molecular structures. The observation of similar orientational behavior in polymer-blend nanoparticles (MEH-PPV and polystyrene), as well as in blends containing a liquid-crystalline polymer, indicate that the behavior is not unique to isolated MEH-PPV but may be applicable to a broad range of polymeric systems confined to nanoscale domains.

Acknowledgment. This research was sponsored by the Division of Chemical Sciences, Office of Basic Energy Sciences, U.S. Department of Energy, under Contract DE-AC05-00OR22725 with Oak Ridge National Laboratory (ORNL), managed and operated by UT-Battelle, LLC. Adosh Mehta acknowledges support of the ORNL Postdoctoral Research Program administered through Oak Ridge Institute of Science and Engineering (ORISE). R. M. Dickson acknowledges financial support from the National Science Foundation (Grant CHE-9984507) and the Alfred P. Sloan Research Foundation and partial support from the Research Corporation and the Georgia Tech Molecular Design Institute (Office of Naval Research Grant N00014-95-1-1116).

References and Notes

(1) Heeger, A. J. *J. Phys. Chem.* B **2001**, *105*, 8475.
(2) Ivanov, V. A.; Paul, W.; Binder, K. *J. Chem. Phys.* **1998**, *109*, 5659.
(3) Tour, J. M. *Acc. Chem. Res.* **2000**, *33*, 791.
(4) Nguyen, T. Q.; Wu, J. J.; Doan, V.; Schwartz, B. J.; Tolbert, S. *Science* **2000**, *288*, 652.
(5) Hu, D.; Yu, L.; Barbara, P. F. *J. Am. Chem. Soc.* **1999**, *121*, 6936.
(6) Vanden Bout, D. A. et al. *Science* **1997**, *277*, 1074.
(7) Huser, T.; Yan, M.; Rothberg, L. J. *Proc. Natl. Acad. Sci. U.S.A.* **2000**, *97*, 11187.
(8) Nguyen, T. Q.; Doan, V.; Schwartz, B. J. *J. Chem. Phys.* **1999**, *110*, 4068−4078.
(9) Schaller, R. D.; Snee, P. T.; Johnson, J. C.; Lee, L. F.; Wilson, K. R.; Haber, L. H.; Nguyen, R. J. T.-Q.; Schwartz, B. J. *J. Chem. Phys.* **2002**, *117*, 6688.

(10) Hu, D.; Yu, L.; Barbara, P. F. *J. Am. Chem. Soc.* **1999**, *121*, 6936−6937.
(11) Yu, J.; Hu, D.; Barbara, P. F. *Science* **2000**, *289*, 1327−1331.
(12) Padmanaban, G.; Ramakrishnan, S. *J. Am. Chem. Soc.* **2000**, *122*, 2244−2251.
(13) Gettinger, C. L.; Heeger, A. J.; Drake, J. M.; Pine, D. J. *J. Chem. Phys.* **1994**, *101*, 1673−1678.
(14) Yip, W. T.; Hu, D. H.; Yu, J.; Vanden Bout, D. A.; Barbara, P. F. *J. Phys. Chem. A* **1998**, *102*, 7564.
(15) Hu, D.; Yu, J.; Bagchi, B.; Rossky, P. J.; Barbara, P. F. *Nature* **2000**, *405*, 1030.
(16) Yu, J.; Hu, D.; Barbara, P. F. *Science* **2000**, *289*, 1327.
(17) Gettinger, C. L.; Heeger, A. J.; Drake, J. M.; Pine, D. J. *J. Chem. Phys.* **1994**, *101*, 1673.
(18) Kung, C.-Y.; Barnes, M. D.; Lermer, N.; Whitten, W. B.; Ramsey, J. M. *Appl. Opt.* **1999**, *38*, 1481.
(19) Barnes, M. D.; Ng, K. C.; Fukui, K.; Sumpter, B. G.; Noid, D. W. *Macromolecules* **1999**, *32*, 7183.
(20) Hellen, E. H.; Axelrod, D. *J. Opt. Soc. Am. B* **1987**, *4*, 337.
(21) Bartko, A. P.; Xu, K.; Dickson, R. M. *Phys. Rev. Lett.* **2002**, *89*, 026101.
(22) Bartko, A. P. et al. *Chem Phys. Lett.* **2002**, *358*, 459.
(23) Bartko, A. P.; Dickson, R. M. *J. Phys. Chem. B* **1999**, *103*, 11237.
(24) Emission patterns were directly measured by imaging the spatial distribution of fluorescence through a 1.4-NA (numerical aperture) 100× oil objective onto a CCD camera. Particle fluorescence was excited with an Ar^+ laser beam (514.5 nm excitation wavelength; intensities 50−500 W/cm^2) aligned within the objective to produce total internal reflection (TIR) at the coverglass−air interface. Fluorescence was collected through the same high NA objective used to focus the excitation light, passed through a dichroic filter with a band-edge (50% transmission) at 530 nm, and imaged with a CCD camera with 45 nm real-space distance per pixel. All measurements were made under ambient atmospheric conditions, except where indicated.
(25) Mehta, A.; Thundat, T.; Barnes, M. D.; Chhabra, V.; Bhargava, R.; Bartko, A. P.; Dickson, R. M. *Appl. Opt.*, in press.
(26) Chang, R. et al. *Chem Phys. Lett.* **2000**, *317*, 142.
(27) Bazan, G.; Oldham, W. J., Jr.; Lachicotte, R. J.; Tretiak, S.; Chernyak, V.; Mukamel, S. *J. Am. Chem. Soc.* **1998**, *120*, 9188.
(28) Detert, H.; Schollmeyer, D.; Sugiono, E. *Eur. J. Org. Chem.* **2001**, 2927−2938.
(29) Barnes, M. D. et al. *Phys. Rev. Lett.* **1996**, *76*, 3931.
(30) Pichler, K.; Halliday, D. A.; Bradley, D. D. C.; Burns, P. L.; Friend, R. H.; Holmes, A. B. *J. Phys.: Condens. Matter* **1993**, *5*, 7155.